

GRAVITATIONAL COLLAPSE OF MAGNETIZED CLOUDS

II. THE ROLE OF OHMIC DISSIPATION

Frank H. Shu

*Physics Department, National Tsing Hua University
 Hsinchu 30013, Taiwan, Republic of China
 shu@mx.nthu.edu.tw*

Daniele Galli

*INAF-Osservatorio Astrofisico di Arcetri
 Largo Enrico Fermi 5, I-50125 Firenze, Italy
 galli@arcetri.astro.it*

Susana Lizano

*Centro de Radioastronomía y Astrofísica, UNAM
 Apdo. Postal 3-72, Morelia, Michoacán 58089, Mexico
 s.lizano@astrosmo.unam.mx*

Mike Cai

*Physics Department, National Tsing Hua University
 Hsinchu 30013, Taiwan, Republic of China
 mike@phys.nthu.edu.tw*

ABSTRACT

We formulate the problem of magnetic field dissipation during the accretion phase of low-mass star formation, and we carry out the first step of an iterative solution procedure by assuming that the gas is in free-fall along radial field lines. This so-called “kinematic approximation” ignores the back reaction of the Lorentz force on the accretion flow. In quasi steady-state, and assuming the resistivity coefficient to be spatially uniform, the problem is analytically soluble in terms of Legendre’s polynomials and confluent hypergeometric functions. The dissipation of the magnetic field occurs inside a region of radius inversely proportional to the mass of the central star (the “Ohm radius”), where the magnetic field becomes asymptotically straight and uniform. In our solution, the magnetic flux problem of star formation is avoided because the magnetic flux dragged in

the accreting protostar is always zero. Our results imply that the effective resistivity of the infalling gas must be higher by several orders of magnitude than the microscopic electric resistivity, to avoid conflict with measurements of paleomagnetism in meteorites and with the observed luminosity of regions of low-mass star formation.

Subject headings: ISM:clouds — ISM: magnetic fields — magnetohydrodynamics — planetary systems: protoplanetary disks — stars: formation

1. Introduction

If the magnetic field of a collapsing interstellar gas cloud remained frozen in the gas, the resulting surface magnetic field of the newborn protostar would exceed observed stellar fields by almost four orders of magnitude (the so-called “magnetic flux problem”, see e.g., Mestel & Spitzer 1956). It follows that the excess magnetic flux of a cloud must be dissipated at some stage during the process of star formation. Assuming ideal magnetohydrodynamic (MHD) conditions, Galli et al. (2006, hereafter Paper I) obtained an analytical solution for the inner regions of an isothermal, magnetized, rotating cloud undergoing gravitational collapse and showed that the long-lever arms of the strong field trapped in the central protostar in a split-monopole configuration would cause so much magnetic braking as to make impossible the formation of a centrifugally supported disk around the central object (see also Allen et al. 2003a,b). Thus, the dissipation of magnetic field must occur prior or simultaneously to the formation of a circumstellar disk. In the current paper, we remove the assumption of field freezing by allowing the non-ideal effect of finite electric resistivity to operate, and we determine the value of the resistivity coefficient required to solve the magnetic flux problem during the accretion phase of low-mass star formation.

The paper is organized as follows: in Section 2 we formulate the basic equations of the problem; in Section 3 we estimate the value of the resistivity coefficient in the central region of collapse from the available observational constraints; in Section 4 we check the validity of our approximations; in Section 5 we compare our results with those of previous works; finally, in Section 6, we summarize our conclusions. The reader not interested to the mathematical derivation of our results, can go directly to eq. (31).

2. Formulation of the problem

Neglecting the effects of ambipolar diffusion (but see Section 6), the evolution of the

magnetic field in a collapsing cloud is governed by the induction equation with ohmic dissipation,

$$\frac{\partial \mathbf{B}}{\partial t} + \nabla \times (\mathbf{B} \times \mathbf{u}) = -\nabla \times (\eta \nabla \times \mathbf{B}), \quad (1)$$

where η is the coefficient of ohmic resistivity, related to the electric conductivity σ by

$$\eta = \frac{c^2}{4\pi\sigma}. \quad (2)$$

Assuming axial symmetry, and a purely poloidal magnetic field, we can “uncurl” eq. (1) and express it in scalar form as

$$\frac{\partial \Phi}{\partial t} + \mathbf{u} \cdot \nabla \Phi = \eta \mathcal{S}(\Phi), \quad (3)$$

where Φ is the flux function, defined in spherical coordinates by

$$\mathbf{B} = \nabla \times \left[\frac{\Phi(r, \theta)}{2\pi r \sin \theta} \hat{\mathbf{e}}_\varphi \right], \quad (4)$$

and \mathcal{S} is the Stokes operator

$$\mathcal{S} \equiv \frac{\partial^2}{\partial r^2} + \frac{1}{r^2} \frac{\partial^2}{\partial \theta^2} - \frac{\cot \theta}{r^2} \frac{\partial}{\partial \theta}. \quad (5)$$

Since B_r is antisymmetric with respect to the midplane, eq. (4) implies that the flux function Φ is even with respect to $\theta = \pi/2$. In addition, because the field is finite on the polar axis (except at the origin), the flux function Φ must vanish for $\theta = 0$ and $\theta = \pi$ ¹

Following Paper I, we assume that the velocity is given by free-fall on a point mass M_\star at the origin,

$$\mathbf{u}(r) = - \left(\frac{2GM_\star}{r} \right)^{1/2} \hat{\mathbf{e}}_r, \quad (6)$$

and we ignore the reaction of the magnetic field on the flow (the validity of this assumption is to be checked a posteriori). Because the dissipation is likely to occur in a region of space across which the flow time is short in comparison with the evolutionary time of the collapse of the molecular cloud core, we may look for a quasi-steady state in which the advection of magnetic flux by the flow is balanced by ohmic dissipation,

$$- \left(\frac{2GM_\star}{r} \right)^{1/2} \frac{\partial \Phi}{\partial r} = \eta \mathcal{S}(\Phi). \quad (7)$$

¹The physical flux threading a circle of radius r on the midplane is given by the value $\Phi(r, \theta = \pi/2)$.

At large r , the flux function must asymptotically approach that of a split monopole,

$$\lim_{r \rightarrow \infty} \Phi(r, \theta) = \Phi_\star(1 - |\cos \theta|), \quad (8)$$

where

$$\Phi_\star = 2\pi\lambda_\star^{-1}G^{1/2}M_\star \quad (9)$$

is the flux trapped by the central protostar, and the parameter λ_\star is the mass-to-flux ratio of the central split monopole in non-dimensional units (see Paper I). Note that λ_\star is a measure of the magnetic flux trapped in the star under ideal MHD condition, and does not correspond to the actual mass-to-flux ratio measured in young stars ($\sim 10^3$ – 10^4 in the same units). In Paper I, we obtained $1 \lesssim \lambda_\star \lesssim 4$ by connecting the analytic inner collapse solution to the ideal MHD numerical models of Allen et al. (2003a,b). In the following, we will use $\lambda_\star \approx 2$ as a fiducial value.

2.1. Nondimensional variables

To be specific and for simplicity, we assume that η is spatially constant and we define the nondimensional variables

$$r = r_{\text{Ohm}}x, \quad \Phi(r, \theta) = \Phi_\star\phi(x, \mu), \quad (10)$$

where $\mu = \cos \theta$ and

$$r_{\text{Ohm}} \equiv \frac{\eta^2}{2GM_\star} \quad (11)$$

is the *Ohm radius*. We may then justify the assumption of a quasi-steady state if the fractional variations of the parameters of the problem, M_\star and Φ_\star , are negligible over a diffusion time

$$t_{\text{Ohm}} \equiv \frac{r_{\text{Ohm}}^2}{\eta} = \frac{\eta^3}{4G^2M_\star^2}. \quad (12)$$

Because advection is balanced against diffusion, the expression (12) is also the time it takes to cross r_{Ohm} at the local free-fall velocity

$$u(r_{\text{Ohm}}) = \left(\frac{2GM_\star}{r_{\text{Ohm}}} \right)^{1/2} = \frac{2GM_\star}{\eta}, \quad (13)$$

which explains why r_{Ohm} is defined as in eq. (11). If we adopt the values $\eta \approx 2 \times 10^{20}$ cm 2 s $^{-1}$ and $M_\star \approx 1 M_\odot$ (see Sect. 3), we get $t_{\text{Ohm}} \approx 3$ yr, which is very short compared to the timescale

$$t_{\text{acc}} \equiv \frac{M_\star}{\dot{M}} \sim 10^5 \text{ yr}, \quad (14)$$

over which we may expect M_\star or Φ_\star to have significant variations. Thus, the quasi-steady approximation is likely to be a good one.

With these definitions, eq. (7) becomes

$$x^2 \frac{\partial^2 \phi}{\partial x^2} + x^{3/2} \frac{\partial \phi}{\partial x} = -(1 - \mu^2) \frac{\partial^2 \phi}{\partial \mu^2}. \quad (15)$$

Setting $\phi(x, \mu) = F(x)G(\mu)$, we reduce eq. (15) by separation of variables to the couple of ordinary differential equations

$$(1 - \mu^2)G'' + \Lambda G = 0, \quad (16)$$

where Λ is a separation constant, and

$$x^2 F'' + x^{3/2} F' - \Lambda F = 0. \quad (17)$$

Differentiating eq. (16) with respect to μ , and setting $g(\mu) = G'(\mu)$, we see that $g(\mu)$ satisfies Legendre's equation,

$$(1 - \mu^2)g'' - 2\mu g' + \Lambda g = 0. \quad (18)$$

Solutions of Legendre's equation regular at $\mu = \pm 1$ require $\Lambda = l(l+1)$, with $l = 0, 1, 2, \dots$, and are given by Legendre's polynomials $P_l(\mu)$ of order l , i.e. $g(\mu) \propto P_l(\mu)$. Using the definition of g and eq. (16), we then obtain $G(\mu) \propto (1 - \mu^2)P'_l(\mu)$. Therefore, any solution of eq. (16) regular on the polar axis can be written as a linear combination of polynomials of degree $n = l + 1$,

$$G_n(\mu) = C_n(1 - \mu^2) \frac{dP_{n-1}}{d\mu} = nC_n[\mu P_{n-1}(\mu) - P_n(\mu)], \quad (19)$$

where C_n are arbitrary constants. Defining

$$C_n \equiv \left[\frac{2n-1}{2n(n-1)} \right]^{1/2}, \quad (20)$$

the polynomials $G_n(\mu)$ form an orthonormal set with weight $(1 - \mu^2)^{-1}$,

$$\int_{-1}^{+1} G_n(\mu) G_m(\mu) \frac{d\mu}{1 - \mu^2} = \delta_{nm}, \quad (21)$$

as can be easily shown by a simple integration by parts and using the normalization condition of Legendre's polynomials. Since the flux function is an even function of μ over the interval $-1 \leq \mu \leq 1$, the index n takes only even values $n = 2, 4, \dots$. Figure 1 shows the functions $G_n(\theta)$ for $n = 2-10$.

The boundary condition (8) must be expanded in terms of G_n polynomials,

$$\lim_{x \rightarrow \infty} \phi(x, \mu) = 1 - |\mu| = \sum_{n=2,4,\dots}^{\infty} f_n G_n(\mu), \quad (22)$$

where f_n are the spectral coefficients. Multiplying both sides of this equation by $G_m(\mu)/(1 - \mu^2)$ and integrating from $\mu = -1$ to $\mu = 1$ we easily obtain, using the orthogonality property (21), and integrating by parts,

$$f_n = 2C_n \int_0^1 P_{n-1}(\mu) \, d\mu = (-1)^{n/2-1} \frac{2(n-1)!!}{n(n-1)(n-2)!!} C_n, \quad (23)$$

where the latter equality follows from a formula in Byerly (1959).

We now turn to eq. (17), with $\Lambda = n(n-1)$. For each n , this equation has to be solved under the boundary conditions

$$F_n = 0 \text{ at } x = 0, \quad \lim_{x \rightarrow \infty} F_n(x) = f_n, \quad (24)$$

where the constants f_n are given by eq. (23). In terms of the new variables z and H_n defined by

$$z = 2\sqrt{x} \quad \text{and} \quad F_n = z^{2n} e^{-z} H_n, \quad (25)$$

eq. (17) becomes Kummer's equation (Abramowitz & Stegun 1965 [13.1.1], hereafter AS65) or *confluent hypergeometric equation* (see e.g. Landau & Lifshitz 1959, Appendix *d*),

$$zH_n'' + (b_n - z)H_n' - a_n H_n = 0, \quad (26)$$

with $a_n = 2n - 1$ and $b_n = 4n - 1$. The general solution of Kummer's equation is (AS65 [13.1.11])

$$H_n(z) = A_n M(a_n, b_n, z) + B_n U(a_n, b_n, z), \quad (27)$$

where A_n and B_n are arbitrary constants, and M , U are called *Kummer's functions* or *confluent hypergeometric functions* of the first and second kind, respectively (regular at the origin, and at infinity, respectively)². For $z = 0$, $M(a_n, b_n, 0) = 1$ whereas $U(a_n, b_n, z)$ diverges like $z^{1-b_n} = z^{-4n}$. The latter behavior implies $F_n \sim x^{-n}$ for small x , in contrast with the boundary condition $F_n(0) = 0$. Therefore $B_n = 0$ and

$$F_n(x) = A_n (2\sqrt{x})^{2n} e^{-2\sqrt{x}} M(2n-1, 4n-1, 2\sqrt{x}). \quad (28)$$

²Kummer's equation describes the radial part of the Coulomb wavefunction. If $a_n \leq 0$, the solutions of Kummer's equation well-behaved at infinity are associated Laguerre's polynomials.

The constants A_n are fixed by imposing the boundary condition at infinity (eq. 24). Since $M(a_n, b_n, z)$ has the asymptotic behavior (AS65 [13.1.4])

$$\lim_{z \rightarrow \infty} M(a_n, b_n, z) = \frac{(b_n - 1)!}{(a_n - 1)!} e^z z^{a_n - b_n}, \quad (29)$$

we immediately obtain

$$A_n = \frac{(2n - 2)!}{(4n - 2)!} f_n. \quad (30)$$

Figure 2 shows the functions $F_n(x)$ for $n = 2-10$.

Combining the angular and radial solutions and summing over n , we finally obtain

$$\phi(x, \mu) = e^{-2\sqrt{x}} \sum_{n=2,4,\dots}^{\infty} K_n x^n M(2n - 1, 4n - 1, 2\sqrt{x}) [\mu P_{n-1}(\mu) - P_n(\mu)] \quad (31)$$

where

$$K_n = (-1)^{n/2-1} \frac{2^{2n} (n-1)!! (2n-1)!}{(n-2)!! (4n-2)! (n-1)^2 n}. \quad (32)$$

The function $M(a_n, b_n, z)$ can be evaluated numerically with standard routines, e.g. the Fortran program CHGM.FOR of Zhang & Jin (1996). For $x \gg 1$ is better to use the full asymptotic expansion eq. (29), given by AS65 [13.5.1]. For $x \ll 1$, the series in eq. (31) is dominated by the $n = 2$ term, and we obtain

$$\lim_{x \rightarrow 0} \phi(x, \theta) = \frac{1}{30} x^2 \sin^2 \theta, \quad (33)$$

corresponding, as expected, to a uniform magnetic field with vertical field lines. Figure 3 shows the flux function $\phi(x, 0)$ in the midplane ($\theta = \pi/2$) given by eq. (31), and its asymptotic behavior given by eq. (33). At the Ohm radius the flux is reduced by a factor ~ 100 with respect to the asymptotic value.

Figure 4a, b, c show the magnetic field lines in the meridional plane of the collapse region at different scales, computed according to eq. (31). The horizontal and vertical axis in each panel are the cylindrical self-similar coordinates, $\varpi = x \sin \theta$ and $z = x \cos \theta$. Panel (a) shows the nearly uniform magnetic field inside the Ohm radius, $(R, z)/r_{\text{Ohm}} < 1$. In this region the series solution eq. (31) yields a good representation with the inclusion of only the first six terms. Panel (b) shows the magnetic field lines in the region $(R, z)/r_{\text{Ohm}} < 10$. In this region the series solution eq. (31) gives a good representation including the first four terms. Panel (c) shows the magnetic field lines in the region $(R, z)/r_{\text{Ohm}} < 100$, showing the asymptotic convergence to the field of a split monopole at large radii. In this region the series solution eq. (31) gives a good representation including the first six terms.

3. Numerical estimates

Eq. (33) implies that the strength of the magnetic field at the center approaches a constant value given in dimensional form by

$$B_c = \frac{\Phi_\star}{30\pi r_{\text{Ohm}}^2}, \quad (34)$$

where Φ_\star and r_{Ohm} are given by eq. (9) and (11), respectively. Substituting these values, we obtain

$$B_c = \frac{4G^{5/2}M_\star^3}{15\lambda_\star\eta^4}, \quad (35)$$

showing that B_c scales with the electric conductivity and stellar mass as $\sigma^4 M_\star^3$, a result that may have interesting consequences for high-mass stars.

To estimate the numerical values of the physical quantities of our model, we assume a given value for the uniform magnetic field B_c inside the dissipation region, and we derive the remaining quantities in terms of B_c . An estimate of the intensity of the constant magnetic field in the central region can be inferred from measurements of remanent magnetization in meteorites. Observed values range from ~ 0.1 G in achondrites to ~ 1 G in carbonaceous chondrites, reaching values up to ~ 10 G in chondrules. It is unclear whether this range of values reflects an actual variation in the strength of the magnetizing source. Chondrules have randomly oriented magnetizations which strongly suggest that they record magnetic fields that predate the accretion of the meteorites, but the measured values are the most uncertain. Achondrites, on the other hand, have the least complicated magnetic mineralogies, but local processes such as impacts may have affected their magnetization history (for reviews, see Stacey 1976, Levy & Sonnet 1978, Cisowski & Hood 1991 and references therein). Hereafter we assume $B_c \approx 1$ G.

From eq. (9) and (34) we obtain the Ohm radius

$$r_{\text{Ohm}} = \left(\frac{G^{1/2}M_\star}{15\lambda_\star B_c} \right)^{1/2} \approx 12 \lambda_\star^{-1/2} \left(\frac{M_\star}{M_\odot} \right)^{1/2} \left(\frac{B_c}{1 \text{ G}} \right)^{-1/2} \text{ AU}, \quad (36)$$

weakly dependent on the values of the parameters.

We note that magnetic fields of strength ~ 1 G, when bent sufficiently outwards (e.g., by X-winds; Shu et al. 2000), can drive disk winds (e.g., Königl & Pudritz 2000). However, disk winds driven from footpoints of 2 to 6 AU will have difficulty acquiring the 200 to 300 km s⁻¹ terminal velocities seen in high-speed jet outflows. Nevertheless, we cannot rule out, on the basis of these considerations, the possibility that slow disk winds co-exist with fast X-winds in YSOs.

The corresponding value for the effective resistivity η from the expression for the Ohm radius (eq. 11) is

$$\eta = \left(\frac{4G^{5/2} M_*^3}{15\lambda_* B_c} \right)^{1/4} \approx 2.2 \times 10^{20} \lambda_*^{-1/4} \left(\frac{M_*}{M_\odot} \right)^{3/4} \left(\frac{B_c}{1 \text{ G}} \right)^{-1/4} \text{ cm}^2 \text{ s}^{-1}, \quad (37)$$

again, weakly dependent on the numerical values of the parameters. With our fiducial values $\lambda_* \approx 2$, $M_* \approx 1 M_\odot$, $B_c \approx 1 \text{ G}$, we obtain $r_{\text{Ohm}} \approx 8.5 \text{ AU}$ and $\eta \approx 2 \times 10^{20} \text{ cm}^2 \text{ s}^{-1}$. This is larger by a few orders of magnitude than estimated values from kinetic theory of the microscopic ohmic resistivity in dense gas and circumstellar disks (see Sect. 6), suggesting that the dissipation of magnetic flux probably occurs by some anomalous diffusion process.

The free-fall velocity at the Ohm radius is $u(r_{\text{Ohm}}) \approx 14 \text{ km s}^{-1}$ and the gas density, for an accretion rate $\dot{M} \approx 10^{-5} M_\odot \text{ yr}^{-1}$, is of the order of 10^9 cm^{-3} . This is lower than the often quoted value of the density at decoupling of $10^{11}\text{--}10^{12} \text{ cm}^{-3}$ (e.g., Nishi, Nakano, & Umebayashi 1991), because our adopted effective resistivity is larger than the conventional electric resistivity.

4. Joule heating rate

The magnetic energy annihilated per unit time and unit volume (Joule heating rate) is

$$\frac{\eta}{4\pi} |\nabla \times \mathbf{B}|^2 = \frac{\eta}{16\pi^3} \left[\frac{\mathcal{S}(\Phi)}{r \sin \theta} \right]^2 = \frac{GM_*}{8\pi^3 \eta r^3 \sin^2 \theta} \left(\frac{\partial \Phi}{\partial r} \right)^2, \quad (38)$$

where we have used eq. (7) to eliminate $\mathcal{S}(\Phi)$. For $x \ll 1$, we can approximate $\phi(x)$ with the asymptotic expression eq. (33), obtaining

$$\frac{1}{x^3 \sin^2 \theta} \left(\frac{\partial \phi}{\partial x} \right)^2 \approx \frac{\sin^2 \theta}{225x}, \quad (39)$$

Inserting this expression in eq. (38) and integrating over a sphere of radius r_{Ohm} centered on the origin, we obtain an approximate estimate of the total energy-dissipation rate

$$\dot{\mathcal{E}} \approx \frac{8G^4 M_*^5}{675\lambda_*^2 \eta^5} \approx 300\lambda_*^{-2} \left(\frac{M_*}{M_\odot} \right)^5 \left(\frac{\eta}{10^{20} \text{ cm}^2 \text{ s}^{-1}} \right)^{-5} L_\odot. \quad (40)$$

The dependence of $\dot{\mathcal{E}}$ on the inverse fifth power of η can be easily understood, since the energy dissipation rate is proportional to the resistivity times the square of the electric current density ($\propto \eta^{-12}$) times the volume ($\propto \eta^6$) in which the current flows (eq. 38). The

increase of the electric current in the limit of small resistivity (as η^{-6}) suggests that the anomalous source of field dissipation could be associated with current-driven instabilities occurring when the drift speed of the charged species becomes larger than the ion's thermal speed, as anticipated by Norman & Heyvaerts (1985).

With our fiducial values we obtain $\dot{\mathcal{E}} \approx 3 L_\odot$, but given the sensitive dependence of $\dot{\mathcal{E}}$ on the uncertain parameter η this number may not be very significant. What is more interesting is that the adopted resistivity, which is high by conventional microscopic standards (see Sect. 6), cannot be much lower without violating observational constraints concerning the total luminosity from regions of low-mass star formation (see the reviews of Evans 1999 or Lada & Lada 2003). For example, decreasing the value of η by a factor of 10, increases the central magnetic field to $B_c \approx 10$ kG, and decreases the Ohm radius to $r_{\text{Ohm}} \approx 0.1$ AU. Although magnetic fields of kilogauss strength are measured on the surface of young stars, the energy-dissipation rate for this reduced value of η increases to $\dot{\mathcal{E}} \approx 3 \times 10^5 L_\odot$, which is unrealistic for solar-mass stars. Imposing the condition that the energy-dissipation rate must be lower than the total accretion luminosity $GM_\star \dot{M}/R_\star$, we obtain a lower limit on the resistivity,

$$\eta \gtrsim \left(\frac{8G^3 M_\star^4 R_\star}{675 \lambda_\star \dot{M}} \right)^{1/5} \approx 10^{20} \left(\frac{M_\star}{M_\odot} \right)^{4/5} \left(\frac{R_\star}{R_\odot} \right)^{1/5} \left(\frac{\dot{M}}{10^{-5} M_\odot \text{ yr}^{-1}} \right)^{-1/5} \text{ cm}^2 \text{ s}^{-1}. \quad (41)$$

Notice also that the energy-dissipation rate $\dot{\mathcal{E}}$ scales with the stellar mass as M_\star^5 , which is steeper than the main-sequence luminosity-mass relation, unless the resistivity increases significantly with increasing M_\star . Such a behavior runs counter to the usual notion that high-mass stars possess more ionizing potential than low-mass stars. Nevertheless, high mass stars are formed with mass accretion rates which are more than 100 times larger than low-mass stars (see, e.g., Osorio, Lizano & D'Alessio 1999). In these conditions of very high circumstellar density the ionization front will be confined to the stellar surface and the penetrating ionizing agent for the pseudodisks and disks will not be ultraviolet photons but cosmic rays and/or X-rays.

5. Validity of the kinematic approximation

To check the validity of the kinematic approximation (i.e. the assumption that the infall velocity is dominated by the gravity of the central star), we evaluate the ratio of the Lorentz force per unit volume in the radial direction

$$F_L = \frac{1}{4\pi} [(\nabla \times \mathbf{B}) \times \mathbf{B}]_r = \frac{\mathcal{S}(\Phi)}{16\pi^3 r^2 \sin^2 \theta} \frac{\partial \Phi}{\partial r}, \quad (42)$$

and the gravitational force per unit volume

$$F_g = \frac{GM_\star\rho}{r^2}, \quad (43)$$

where the density is

$$\rho = \frac{\dot{M}}{4\pi r^2|u(r)|}Q(\theta), \quad (44)$$

and $Q(\theta)$ yields the flattening of density contours because of pinching forces associated with the radial magnetic field (see Paper I). The ratio of the two forces is

$$\frac{|F_L|}{|F_g|} = \lambda_\star^{-2} \left(\frac{t_{\text{acc}}}{t_{\text{Ohm}}} \right) \left(\frac{\partial\phi}{\partial x} \right)^2 \frac{x}{Q(\theta) \sin^2 \theta}, \quad (45)$$

where we have used eq. (7) to eliminate $\mathcal{S}(\Phi)$ and we used eqs. (12) and (14). The RHS is proportional to the ratio of two characteristic times, the accretion time, $t_{\text{acc}} \approx 10^5$ yr, and the crossing time of the ohmic dissipation region, $t_{\text{Ohm}} \approx 3$ yr. The validity of the kinematic approximation is nevertheless ensured by the fact that the function of x and θ on the right of this expression is very small. Figure 4d shows contours of the ratio $|F_L|/|F_g|$ computed with the function $Q(\theta)$ corresponding to the case $H_0 = 1$ of Paper I. Notice that the force ratio is low precisely in the equatorial regions where we might expect the formation of a centrifugally supported disk to take place if we had included the effects of angular momentum in the problem.

We also stress that the ratio of the Lorentz and gravitational forces given by eq. (45) depends on resistivity as η^{-3} . As our solution clearly shows, the non-zero resistivity of the gas results in a release of the field from the central protostar, as the gravitational pull of the central star is no longer fully available to pin the magnetic field of the central regions. However, the released magnetic field can be too strong for gravity to continue to win over the Lorentz force. If η is sufficiently large, gravity dominates, and quasi-steady accretion onto the central source is possible. If η is too small, magnetic forces overwhelm gravity, and the accretion region might try to explode outwards. If the coefficient of resistivity can reach anomalous values, the explosion outwards (when η is small) may be coupled with re-implosion inwards when η later becomes (anomalously) large. It is interesting to speculate that these alternating reconnection behaviors (“flares”) might correspond to FU-Orionis outbursts. This mechanism may be an alternate explanation to the disk thermal instability, possibly aided by protoplanet or protostellar companions, which has been proposed for the FU-Orionis phenomenon (e.g., Kawazoe & Mineshige 1993; Bell et. al 1995; Clarke & Syer 1996).

6. Comparison with other works

According to calculations by Stepinski (1992) the electrical resistivity in the presolar nebula in the range of radii 3–30 AU is in the range from $\sim 10^{17}$ to $\sim 10^{16}$ cm 2 s $^{-1}$ if the grain size is ~ 1 cm, or from $\sim 10^{19}$ to $\sim 10^{16}$ cm 2 s $^{-1}$ if the grain size is $0.5\ \mu\text{m}$. Clearly, the physical conditions in a disk are different from those of our infall model. Wardle & Ng (1999) have evaluated the components of the conductivity tensor for molecular gas for a variety of grain models, as function of the gas density. At our fiducial value of $n(\text{H}_2) \approx 10^9$ cm $^{-3}$, they predict a ohmic resistivity $\eta \approx 10^{16}$ cm 2 s $^{-1}$ for a standard grain-size distribution, much lower than our value $\eta \approx 10^{20}$ cm 2 s $^{-1}$. Therefore, the work of Stepinski (1992) and Wardle & Ng (1999) suggest that the effective resistivity η of the infalling gas had better be larger than the microscopic electric resistivity, or severe conflicts with observational data arise. Given the precedent in solar physics, this result does not come totally unexpected. Unlike the solar case, however, the required increase in “anomalous” resistivity may not be huge, if the dust grains in the infalling envelopes of protostars, in contrast with those in protostellar disks, have not undergone too much growth.

Desch & Mouschovias (2001) consider the dissipation of the magnetic field in a collapsing molecular cloud core, during the pre-pivotal stage of evolution ($t < 0$). Because no central star is present in the calculations of Desch & Mouschovias (2001), the velocity field and the density profile clearly differ from the free-fall behavior assumed in this work. The equation for the evolution of the magnetic field has the same form as in this work, but Desch & Mouschovias (2001) also include in the resistivity η also the contribution of ambipolar diffusion,

$$\eta = \eta_{\text{Ohm}} + \eta_{\text{AD}}. \quad (46)$$

The latter is given by

$$\eta_{\text{AD}} = \frac{|\nabla\Phi|^2}{16\pi^3\gamma\rho_i\rho_n r^2 \sin^2\theta} = \frac{|\mathbf{B}|^2}{4\pi\gamma\rho_i\rho_n}, \quad (47)$$

where ρ_i and ρ_n are the mass density of ions and neutral, respectively, and γ is the ion-neutral drag coefficient. The numerical calculations of Desch & Mouschovias (2001) seem to suggest that the magnetic field approaches a steady-state configuration towards the end of the run, characterized by a nearly uniform magnetic field of strength ≈ 0.1 G over a central region of size ≈ 20 AU. Outside this region, the field decreases approximately as r^{-1} , as for field-freezing in a quasi-static isothermal envelope (Li & Shu 1996), whereas in our case of post-pivotal state evolution ($t > 0$) the field decreases like r^{-2} , as for a split monopole. In the region of nearly uniform field (for density larger than $\approx 10^{12}$ cm $^{-3}$), the ambipolar diffusion resistivity η_{AD} reaches $\approx 10^{20}$ cm 2 s $^{-1}$, and is larger by one order of magnitude than the ohmic resistivity (their Fig. 1b). Thus Desch & Mouschovias (2001) conclude that

ambipolar diffusion is entirely responsible for the dissipation (or better redistribution) of the magnetic flux carried by the infalling gas. We note, however, that the region of uniform field in their model contains a negligible mass ($\approx 0.01 M_\odot$). Once the core enters the post-pivotal phase of dynamical collapse, having dissipated the field in such a tiny fraction of the core’s mass is of little help with respect to solving the magnetic flux problem of star formation.

Nakano, Nishi, & Umebayashi (2002), criticized the results of Desch & Mouschovias (2001) noticing that they neglected the (dominant) contribution of grains to the ambipolar diffusion resistivity. Including the grain contribution, Nakano et al. (2002) found a much smaller value of the ambipolar diffusion resistivity than Desch & Mouschovias (2001) and concluded that for densities above $\approx 10^{12} \text{ cm}^{-3}$ the field is dissipated by ohmic resistivity. To make progress, future theoretical calculations need to study the complex relationships among field dissipation, disk formation, and grain growth, as well as to include self-consistently the back reaction of the magnetic field and its momentum and energy inputs into the gas as the field is dissipated.

An interesting question is the relative importance of ambipolar diffusion and ohmic dissipation in protostellar accretion flows. The ratio of the ambipolar diffusion time to the ohmic dissipation time is given by

$$\frac{t_{\text{AD}}}{t_{\text{Ohm}}} = \frac{\eta}{v_A^2 \tau_{in}} = \eta \frac{4\pi\gamma\rho_i\rho_n}{B^2}, \quad (48)$$

where $v_A = B/(4\pi\rho_n)^{1/2}$ is the Alfvén speed in the neutrals, and $\tau_{in} = (\gamma\rho_i)^{-1}$ is the ion-neutral collision timescale. Notice that the ratio of timescales depends on the inverse square of the magnetic field. Thus, as the field is weakened, electric resistivity will ultimately dominate the end stages of the process. Indeed, the Ohmic term is the only one of the three conventionally invoked mechanisms for dissipating magnetic fields that is linear in \mathbf{B} in the induction equation (the so-called Hall term is quadratic and the ambipolar diffusion is cubic, see e.g. Cowling 1957). This means that Hall and ambipolar diffusion can never completely annihilate \mathbf{B} ; only Ohmic dissipation can do that.

Because the induction equation (1) with only Ohmic dissipation included is linear in \mathbf{B} , the superposition principle allows us to modify the approach taken in this paper and adapt it to other scenarios. If the process of ambipolar diffusion and ohmic dissipation occur in series as the gas flows inward, then, the compressed core field will be less than the ideal value due to the effect of ambipolar diffusion in the outer regions. Adopting the inner limit of the outer region as the outer limit of our inner calculation, everything then goes through as before. One would just have somewhat different coefficients for the angular functions in eq. (23) and, more importantly, an overall reduction of the effective flux at “infinity”, and thus, an increase in λ_\star . For example, an increase of the mass-to-flux ratio by

ambipolar diffusion by two orders of magnitude, as found by Tassis & Mouschovias (2005a,b), implies $\lambda_\star \sim 200$. From equation (37), the electric resistivity decreases by a factor of ~ 4 . Then, from equation (36), one obtains $r_{\text{Ohm}} \approx 1$ AU. The most important reduction is that the reconnection luminosity decreases substantially to mean levels $\dot{\mathcal{E}} \approx 0.02L_\odot$, a small fraction of the bolometric luminosity, unless the reconnection events occur not steadily but in infrequent, powerful flares. Finally, since this paper argues that Ohmic dissipation operates in the innermost region, the annihilation of the elastic “core” that appears as the bottom-most cell in the calculations of Tassis & Mouschovias (2005a,b) may erode the base from which are launched outwardly propagating shockwaves for their “spasmodic accretion oscillations”. The point is that the inwardly advected magnetic flux past the “last zone” is not simply accumulated, as assumed in their calculations, but systematically destroyed.

7. Summary and conclusions

Assuming quasi-steady state and a spatially uniform resistivity coefficient η , we have solved the problem of magnetic field dissipation during the accretion phase of star formation. We have adopted the velocity field determined in a previous study of the gravitational collapse of a magnetized cloud (Galli et al. 2006), and we have ignored the back reaction of the changed magnetic topology on the flow (using the field-freezing calculations to provide what we have called a “kinematic approximation”). With these assumptions, we have solved the problem analytically, and checked *a posteriori* the validity of our approximations. According to our solution, the magnetic field morphology changes from radial at large distances to asymptotically uniform approaching the origin, so that the magnetic flux accreted by the central star is zero at any time.

To determine the value of the resistivity coefficient η we have considered the restrictions imposed by measurements of magnetic fields in meteorites. These constraints require an effective resistivity $\eta \approx 10^{20} \text{ cm}^2 \text{ s}^{-1}$, probably several orders of magnitude larger than the microscopic electric resistivity of the infalling gas. Having shown that ohmic resistivity can dissipate enough magnetic field to solve the magnetic flux problem satisfying the available observational constraints, one now needs to solve the full dynamic problem of magnetic field dissipation and formation of a centrifugally supported protoplanetary disk in a self-consistent way.

DG and SL acknowledge financial support from the Theoretical Institute for Advance Research in Astrophysics (TIARA), CRyA/UNAM, DGAPA/UNAM and CONACyT (Mexico), and INAF-Osservatorio Astrofisico di Arcetri (Italy), where parts of the research pre-

sented in this paper were done. These authors are also grateful for the warm hospitality of members and staff of these institutions. The research work of FS and MC in Taiwan is supported by the grant NSC92-2112-M-001-062.

REFERENCES

Allen, A., Shu, F. H., & Li, Z.-Y. 2003a, *ApJ*, 599, 351

Allen, A., Li, Z.-Y., & Shu, F. H. 2003b, *ApJ*, 599, 363

Abramowitz, M., Stegun, I. A. 1965, *Handbook of mathematical functions* (New York: Dover), p. 504

Bell, K. R., Lin, D. N. C., Hartmann, L. W., & Kenyon, S. J. 1995, *ApJ*, 444, 376

Byerly, W. E. 1959, *An elementary treatise on Fourier's series, and spherical, cylindrical, and ellipsoidal harmonics, with applications to problems in mathematical physics* (New York: Dover), p. 144

Clarke, C. J., & Syer, D. 1996, *MNRAS*, 278, L23

Cisowski, S. M., Hood, L. L. 1991, in *The Sun in time*, ed. C. P. Sonnet, M. S. Giampapa, & M. S. Matthews (Tucson: University of Arizona Press), p. 761

Cowling, T. G. 1957, *Magnetohydrodynamics* (New York: Interscience Publishers), p. 110

Desch, S. J., & Mouschovias, T. C. 2001, *ApJ*, 550, 314

Evans, N. J. 1999, *ARA&A*, 37, 311

Galli, D., Lizano, S., Shu, F. H., Allen, A. 2006, *ApJ*, submitted (Paper I)

Kawazoe, E., & Mineshige, S. 1993, *PASJ*, 45, 715

Konigl, A., & Pudritz, R. E. 2000, *Protostars and Planets IV*, 759

Lada, C. J., Lada, E. 2003, *ARA&A*, 41, 57.

Landau, L. D., Lifshitz, E. M. 1959, *Quantum Mechanics, non-relativistic theory* (London: Pergamon), §36, and Appendix *d*

Levy, E. H., Sonett, C. P. 1978, in *Protostars & Planets*, T. Gehrels ed. (Tucson: University of Arizona Press), p. 516

Li, Z.-Y., Shu, F. H. 1996, *ApJ*, 472, 211

Mestel, L., & Spitzer, L. 1956, *MNRAS*, 116, 503

Nakano, T., Nishi, R., & Umebayashi, T. 2002, *ApJ*, 573, 199

Nishi, R., Nakano, T., & Umebayashi, T. 1991, *ApJ*, 368, 181

Norman, C., & Heyvaerts, J. 1985, *A&A*, 147, 247

Osorio, M., Lizano, S., & D’Alessio, P. 1999, *ApJ*, 525, 808

Shu, F. H., Najita, J. R., Shang, H., & Li, Z.-Y. 2000, *Protostars and Planets IV*, 789

Stacey, F. D. 1976, *Annual Review of Earth and Planetary Sciences*, 4, 147

Stepinski, T. F. 1992, *Icarus*, 97, 130

Tassis, K., & Mouschovias, T. C. 2005a, *ApJ*, 618, 769

Tassis, K., & Mouschovias, T. C. 2005b, *ApJ*, 618, 783

Wardle, M., & Ng, C. 1999, *MNRAS*, 303, 239

Zhang, S., & Jin, J. 1996, *Computation of special functions* (New York: Wiley), p. 385

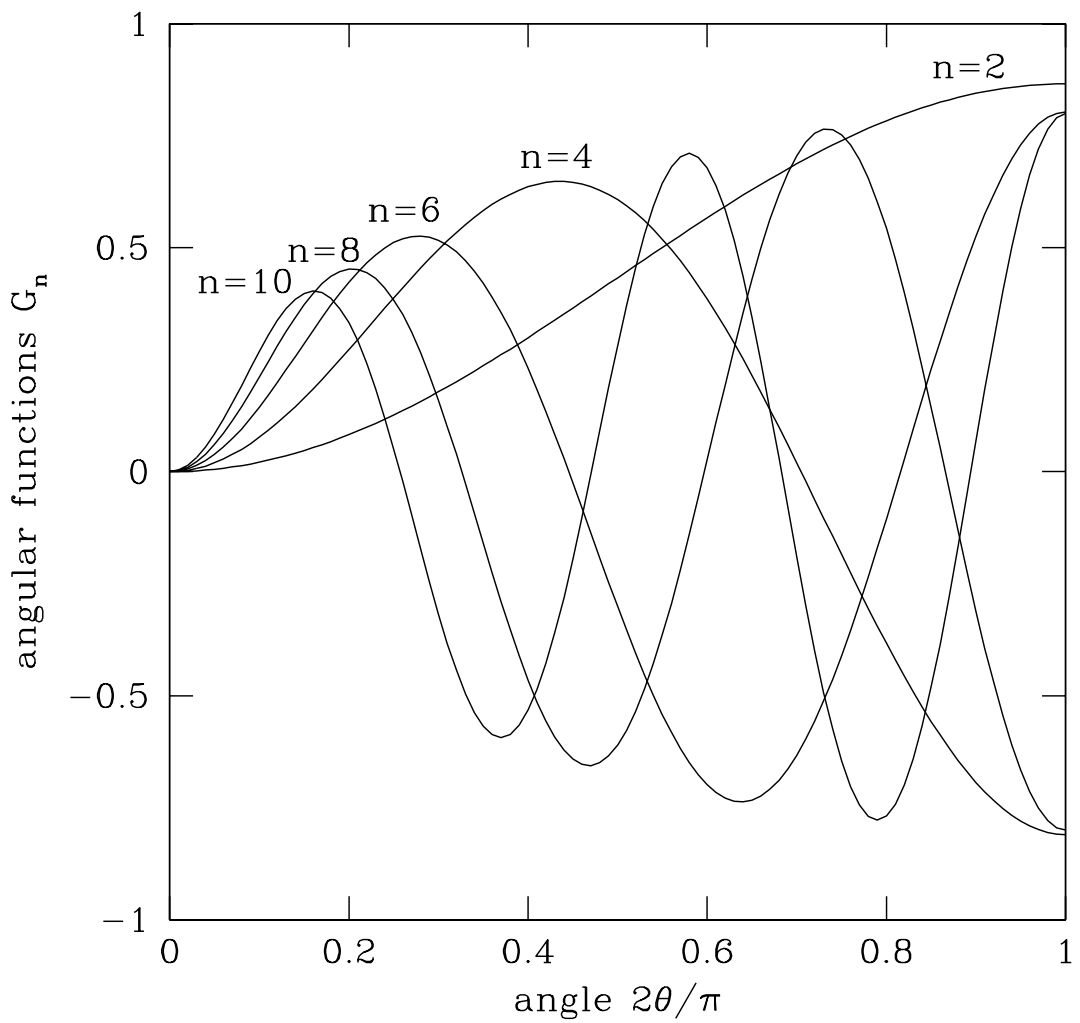


Fig. 1.— The angular functions $G_n(\theta)$ for $n = 2, 4, 6, 8$, and 10 .

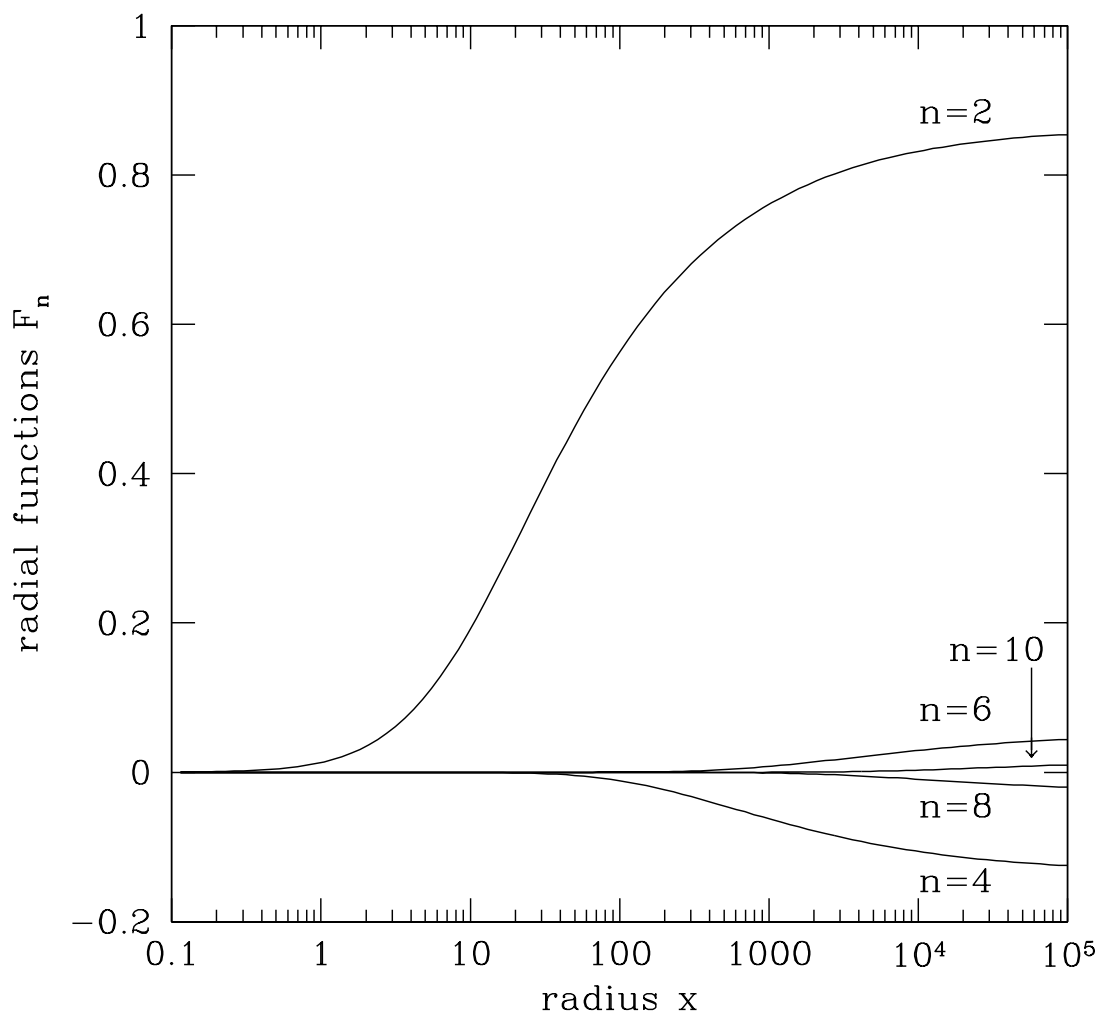


Fig. 2.— The radial functions $F_n(x)$ for $n = 2, 4, 6, 8$, and 10 .

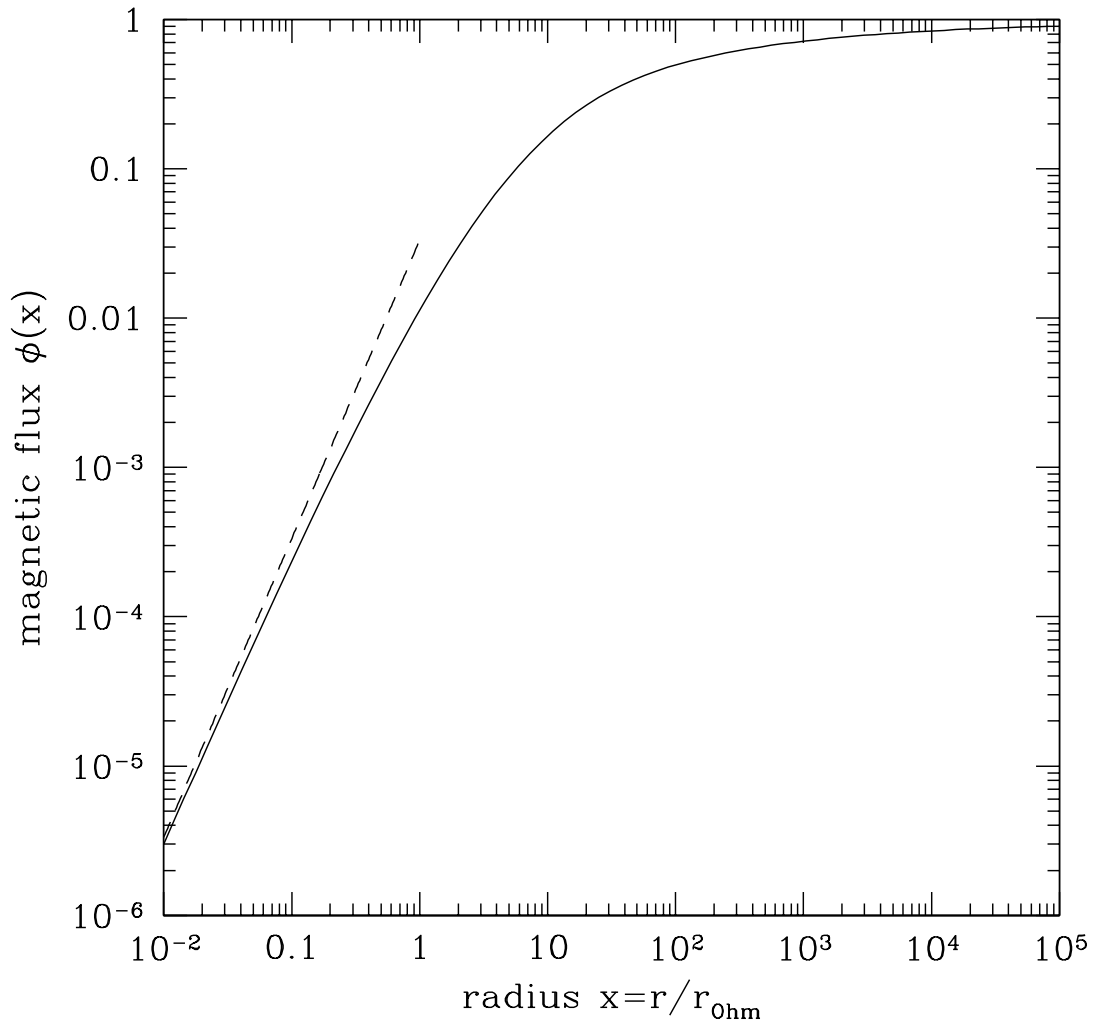


Fig. 3.— The flux function ϕ in the midplane ($\theta = \pi/2$) as function of the distance from the star, in nondimensional units (*solid line*). The *dashed line* shows the uniform field solution given by eq. (33) valid for $x \ll 1$.

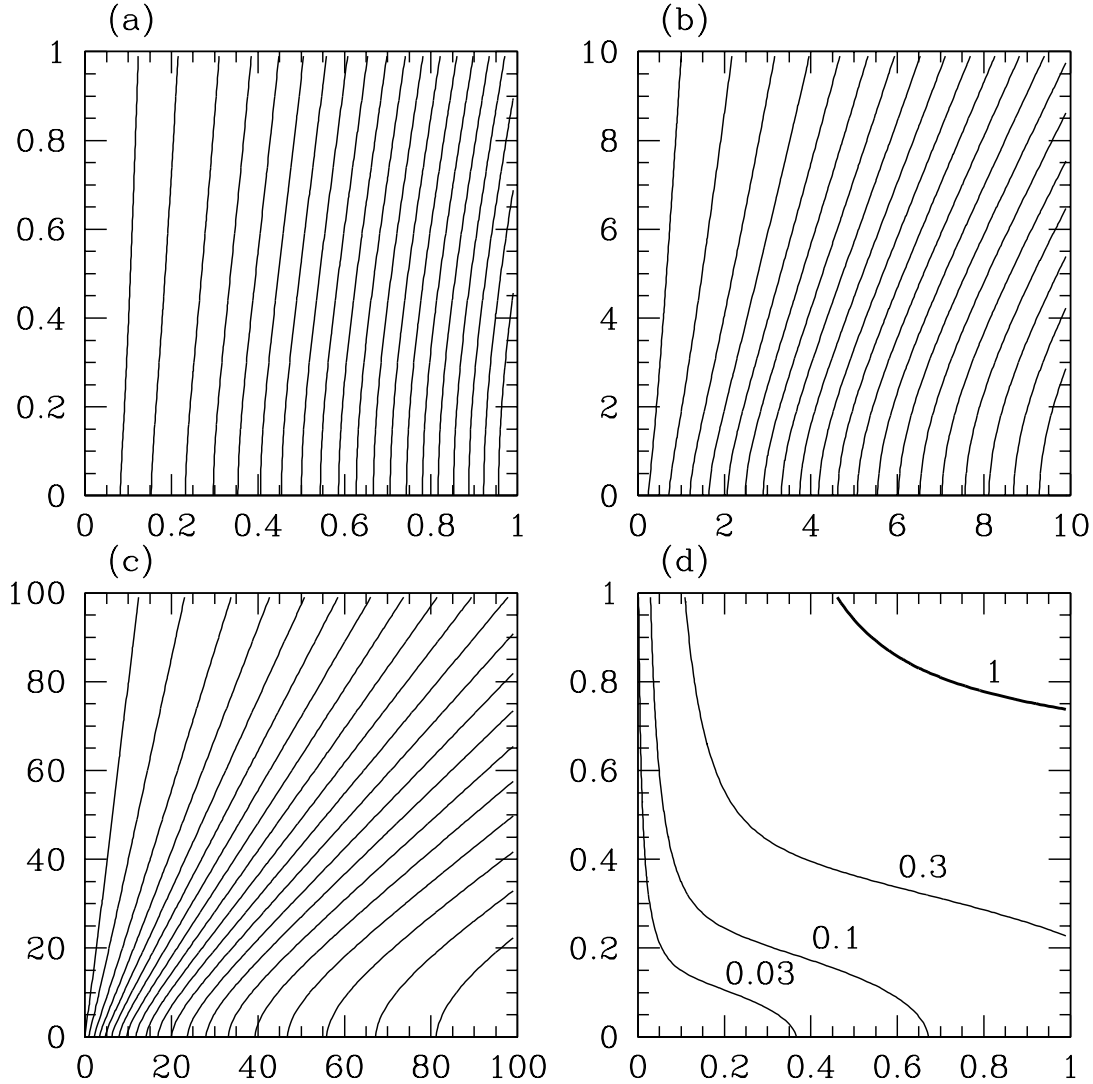


Fig. 4.— (a) The nearly uniform magnetic field inside the Ohm radius, $(\varpi, z)/r_{\text{Ohm}} < 1$. The horizontal and vertical axis in each panel are the cylindrical self-similar coordinates, $\varpi = x \sin \theta$ and $z = x \cos \theta$. (b) Same as (a) in the region $(\varpi, z)/r_{\text{Ohm}} < 10$. (c) Same as (a) in the region $(\varpi, z)/r_{\text{Ohm}} < 100$, showing the asymptotic convergence to the field of a split monopole at large radii. (d) Contours of the ratio $|F_L|/|F_g|$ (Lorentz and gravitational forces) for the density profile corresponding to the collapse of the $H_0 = 0.5$ toroid (see Paper I) in the region $(\varpi, z)/r_{\text{Ohm}} < 1$. The kinematic approximation is formally valid in the region below the *solid curve*. The values of the parameters are $M_* = 0.5 M_\odot$, $\dot{M} = 2 \times 10^{-5} M_\odot \text{ yr}^{-1}$, $\lambda_* = 1.7$.